Structural Engineering and Mechanics, Vol. 5, No. 6 (1997) 705-713
DOI: http://dx.doi.org/10.12989/sem.1997.5.6.705

Boundary element analysis of singular thermal stresses in a unidirectional laminate

Sang Soon Lee† and Beom Shig Kim‡

Reactor Mechanical Engineering Department, Korea Atomic Energy Research Institute, Taejon 306-600, Korea

Abstract. The residual thermal stresses at the interface corner between the elastic fiber and the viscoelastic matrix of a two-dimensional unidirectional laminate due to cooling from cure temperature down to room temperature were studied. The matrix material was assumed to be thermorheologically simple. The time-domain boundary element method was employed to investigate the nature of stresses on the interface. Numerical results show that very large stress gradients are present at the interface corner and this stress singularity might lead to local yielding or fiber-matrix debonding.

Key words: boundary element method; singular thermal stress.

1. Introduction

Residual thermal stresses introduced into fiber-reinforced composites can have a major effect on the microstresses present in such materials. Such stresses are due to the differences between the thermal expansion coefficients of the components. Residual thermal stresses may cause distortion of finished components and premature failure upon tensile loading.

Residual stresses in fiber-reinforced composites have received much attention. A linear elastic stress analysis shows that the residual thermal stresses may be large enough to cause ply failure in the absence of applied external stress or premature failure upon external loading (Hahn and Pagano 1975, Hahn 1976, and Kim and Hahn 1979). Griffin, Jr. (1983) has performed a three-dimensional finite element analysis of residual thermal stresses in symmetric cross-ply laminates with temperature-dependent properties. The assumption of linear elastic behavior, however, tends to overestimate the residual stresses by ignoring the time and temperature dependence of the resin's response. As several investigators have indicated, the matrix has viscoelastic properties during cure (Roy and Murthy 1976, Weitsman 1979, Weitsman and Harper 1982, and Lee and Sohn 1994). Residual stresses may be reduced by changing the cool-down path in a cure cycle because the resin is inherently viscoelastic. Therefore, any analytical model predicting residual stresses in composite laminates must incorporate the viscoelastic response of the matrix resin.

In this study, the residual thermal stresses at the interface corner between the elastic fiber and the viscoelastic matrix of a two-dimensional unidirectional laminate due to cooling from

† Senior Researcher
‡ Principal Researcher

the cure temperature down to room temperature are investigated. A graphite/epoxy laminate was selected and thermorheologically simple material behavior for matrix was assumed. A unidirectional laminate is usually not used in structural components due to the low strength in the transverse direction. In order to be optimal for all external loading conditions, a multidirectional laminate is employed in structural application. A detailed investigation of a unidirectional laminate problem is the first step to solving the more complex problem of a multidirectional laminate. A detailed analysis is performed by using the time-domain boundary element method (BEM) proposed by Lee and Westmann (1995).

2. Analysis model

Fig. 1(a) shows a unidirectional laminate, idealized as an infinite layered solid, and Fig. 1(b) represents the two-dimensional plane strain model for analysis of the microstresses at the interface corner due to cooling from cure temperature down to room temperature. In this study, the fiber volume fraction is assumed to be 0.5. To apply the two-dimensional boundary element technique to the interface stress analysis, the following additional assumptions are made:

1) The fiber-matrix bond is perfect without any defects or any cracks.
2) For sufficiently thin layers and slow fluctuations of the ambient temperature, the transient

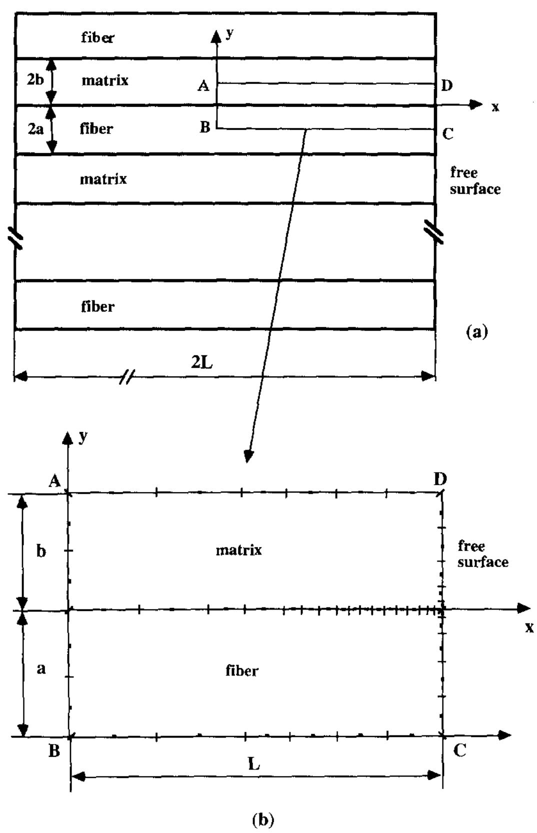

Fig. 1 Idealized model.

state throughout the thickness is neglected resulting in the quasi-static case of uniform temperature $T(x, t) \approx T(t)$ during the cooling down process.

The analysis model of Fig. 1(b) is divided into two subdomains, one matrix zone and one fiber zone; in each zone the material is isotropic and homogeneous. This problem can be treated using a viscoelastic boundary integral formulation for the matrix zone and a separate elastic boundary integral formulation for the fiber zone. These boundary integral equations formulated for every homogeneous zone plus the displacement continuity and traction equilibrium conditions over the common interface produce a system that can be solved once the external boundary conditions are considered.

3. Boundary element formulation

It is assumed that the fibers are linearly elastic while the matrix is linearly viscoelastic in tension and elastic in bulk. The material properties of the fiber are considered to be constant, while the matrix material is assumed to be thermorheologically simple.

The uniform temperature changes $T(t)H(t)$ in each zone of analysis model are equivalent to increasing the tractions by $\gamma^f T(t) n_k$ and $\gamma^m \Theta(t) n_k$ where

$$\begin{aligned} \gamma^f &= 3K^f \alpha^f \\ \gamma^m &= 3K^m \alpha_0 \end{aligned} \tag{1}$$

and $H(t)$ is the Heaviside unit step function. Here superscripts 'f' and 'm' represent the fiber and matrix zones, respectively, K is the bulk modulus, n_k are the components of the unit outward normal to the boundary surface, and α is the coefficient of thermal expansion.

The "pseudo-temperature" $\Theta(t)$ and α_0 are defined by

$$\Theta(t) = \frac{1}{\alpha_0} \int_{T_0}^{T(t)} \alpha^m (T')\, dT' \tag{2}$$

$$\alpha_0 = \alpha^m (T_0)$$

where α^m is the coefficient of the thermal expansion of the matrix.

The fundamental solutions for a viscoelastic body in an isothermal state can be obtained from the solutions of Kelvin's problem of elasticity by applying the elastic-viscoelastic correspondence principle (Lee 1995). With a uniform temperature change in thermorheologically simple media, it is convenient to use the Laplace transform with respect to reduced time ξ, instead of real time t. In effect, the viscoelastic fundamental solutions are obtained in reduced time space. Assuming that no body forces exist, the boundary integral equations for the model under uniform temperature change can be written as follows:
for the fiber zone

$$\begin{aligned} &c_{ij}^f(y)\,\hat{u}_j^f(y, \xi) + \int_{S^f} \hat{u}_j^f(y', \xi)\, T_{ij}^f(y, y')\, dS^f(y') \\ &= \int_{S^f} \hat{t}_j^f(y', \xi)\, U_{ij}^f(y, y')\, dS^f(y') + \int_{S^f} \gamma^f \hat{T}(\xi)\, n_j U_{ij}^f(y, y')\, dS^f(y') \end{aligned} \tag{3}$$

for the matrix zone

$$
\begin{aligned}
&c_{ij}^{m}(\boldsymbol{y})\,\hat{u}_j^{m}(\boldsymbol{y},\ \xi)\\
&+\int_{S^m}\left[\hat{u}_j^{m}(\boldsymbol{y}',\ \xi)\,T_{ij}^{m}(\boldsymbol{y},\ \boldsymbol{y}';0+)+\int_{0+}^{\xi}\hat{u}_j^{m}(\boldsymbol{y}',\ \xi\text{-}\xi')\frac{\partial T_{ij}^{m}(\boldsymbol{y},\ \boldsymbol{y}';\ \xi')}{\partial \xi'}d\xi'\right]dS^m(\boldsymbol{y}')\\
&=\int_{S^m}\left[\hat{t}_j^{m}(\boldsymbol{y}',\ \xi)\,U_{ij}^{m}(\boldsymbol{y},\ \boldsymbol{y}';0+)+\int_{0+}^{\xi}\hat{t}_j^{m}(\boldsymbol{y}',\ \xi\text{-}\xi')\frac{\partial U_{ij}^{m}(\boldsymbol{y},\ \boldsymbol{y}';\ \xi')}{\partial \xi'}d\xi'\right]dS^m(\boldsymbol{y}')\\
&+\int_{S^m}\left[\gamma^m\,\hat{\Theta}(\xi)\,\mathrm{n}_j U_{ij}^{m}(\boldsymbol{y},\ \boldsymbol{y}';0+)+\int_{0+}^{\xi}\gamma^m\,\hat{\Theta}(\xi\text{-}\xi')\,n_j\frac{\partial U_{ij}^{m}(\boldsymbol{y},\ \boldsymbol{y}';\ \xi')}{\partial \xi'}d\xi'\right]dS^m(\boldsymbol{y}')
\end{aligned}
\tag{4}
$$

where $\hat{u}_j$ and $\hat{t}_j$ denote the displacement vector and the traction vector in reduced time space, respectively, and S is the boundary of the given domain. $c_{ij}(\boldsymbol{y})$ is dependent only upon the local geometry of the boundary. For $\boldsymbol{y}$ on a smooth surface, the free-term $c_{ij}(\boldsymbol{y})$ is simply a diagonal matrix 0.5 δ_{ij}. U_{ij} and T_{ij} represent the fundamental solutions and

$$
\xi=\int_0^t\frac{1}{a_T[T(\lambda)]}\,d\lambda,\quad \xi'=\int_0^{t'}\frac{1}{a_T[T(\lambda)]}\,d\lambda \tag{5}
$$

The shift function $a_T(T)$ is a basic property of the material and must, in general, be determined experimentally.

Closed-form integrations of Eqs. (3) and (4) are not, in general, possible and therefore numerical quadrature must be used. Approximations are required in both time and space. Eqs. (3) and (4) can be solved in a step-by-step fashion in time by using the modified Simpson's rule for time integrals and employing the standard BEM for the surface integrals (Lee and Westmann 1995).

The resulting systems of equations are obtained in the matrix form as follows:

$$
\begin{bmatrix} \boldsymbol{H}^1 & \boldsymbol{H}^2 & 0 & \boldsymbol{G}^{12} \\ 0 & \boldsymbol{H}^{21} & \boldsymbol{H}^2 & -\boldsymbol{G}^{21} \end{bmatrix}
\begin{Bmatrix} \boldsymbol{u}^1 \\ \boldsymbol{u}^{12} \\ \boldsymbol{u}^2 \\ \boldsymbol{t}^{21} \end{Bmatrix}
=\begin{bmatrix} \boldsymbol{G}^1 & 0 \\ 0 & \boldsymbol{G}^2 \end{bmatrix}
\begin{Bmatrix} \boldsymbol{t}^1 \\ \boldsymbol{t}^2 \end{Bmatrix}
=\begin{Bmatrix} \boldsymbol{B}_T^1 \\ \boldsymbol{B}_T^2+\boldsymbol{R} \end{Bmatrix}
\tag{6}
$$

In Eq. (6), superscripts '1' and '2' represent the fiber zone and the matrix zone, respectively, while '12' and '21' represent the common interface. $\boldsymbol{H}$ and $\boldsymbol{G}$ are influence matrices, $\boldsymbol{B}_T$ is the known input due to temperature change, and $\boldsymbol{R}$ represents known viscoelastic input from earlier time steps. The above Eq. (6) can be solved by taking account of the external boundary conditions. The length L of the analysis model is taken as $2.5a$. The boundary conditions for the model are given as follows:

$$
\begin{aligned}
&\tau_{xy}=0,\ u_x=0 && \text{along } A\text{-}B\\
&\tau_{xy}=0,\ u_y=0 && \text{along } B\text{-}C\\
&\tau_{xy}=0,\ \sigma_{xx}=0 && \text{along } C\text{-}D\\
&\int_L \sigma_{yy}\,dL=0,\ \tau_{xy}=0,\ u_y=c && \text{along } D\text{-}A
\end{aligned}
\tag{7}
$$

where the integral expression for line D-A represents the traction equilibrium condition on that line. L denotes the length of line D-A, and c represents unknown uniform displacement. Normal displacements of lines A-B and B-C are prescribed as zero to prevent rigid body motion of the model. Due to the symmetry of the model, the shear stresses on every line are zero.

The two-dimensional BEM requires two traction components and two displacement components to be prescribed at each node on the external boundary. As shown in Eq. (7), only one component of tractions is prescribed and normal components of tractions and displacements are given as equilibrium condition and displacement constraint condition on line *D-A*. To enforce Eq. (7), the BEM computer program should be modified.

Let the total number of nodes on line *D-A* be N, then the integral expression for line *D-A* can be written as follows:

$$\int_L \sigma_{yy} dL = \sum_{i=1}^{N} b_i (\sigma_{yy})_i = 0 \tag{8}$$

where $(\sigma_{yy})_i$ represents the normal traction at each node on the line *D-A*, and b_i is the coefficient.

Displacement constraint condition can be written as follows:

$$(u_y)_1 = (u_y)_2 = (u_y)_3 = \cdots\cdots = (u_y)_N = c \tag{9}$$

where $(u_y)_i$ $(i = 1, 2, 3, \cdots, N)$ represents the normal displacement at each node on line *D-A*. The BEM computer program has been modified to include the above equation.

The properties for the matrix are from experimental data (Weitsman 1979):

$$\begin{aligned} E^m(\xi) &= \frac{3.2\times 10^3}{1+0.0336\,\xi^{0.19}}\ \text{MPa} \quad (\xi\text{: min}) \\ K^m(\xi) &= K_0 = 3.556\times 10^3\ \text{MPa} \\ a_T &= \exp\left[\frac{6480}{T} - 21.82\right] \\ \alpha^m &= 0.5\times 10^{-4}\ ℃^{-1} \end{aligned} \tag{10}$$

The following material properties for the fiber were assumed

$$\begin{aligned} K^f &= 2.24\times 10^5\ \text{MPa} \\ \nu^f &= 0.29 \\ \alpha^f &= 0 \end{aligned} \tag{11}$$

If the temperature drops linearly between cure temperature T_0 and room temperature T_r over a time interval t_r then

$$T(t) = \frac{(T_r - T_0)\,t}{t_r} \quad (t\text{: min}) \tag{12}$$

In this study, $t_r = 45$ min, $T_0 = 165℃$, and $T_r = 24℃$ were taken.

To solve the boundary integral Eq. (4), the viscoelastic fundamental solutions, U_{ij}^m and T_{ij}^m, should be known. The relaxation function $E^m(\xi)$, as given in Eq. (10), can be expanded by employing a collocation scheme as

$$E^m(\xi) = E_0 + \sum_{i=1}^{14} E_i \exp\left(-\frac{\xi}{\lambda_i}\right) \tag{13}$$

The numerical values of E_i and λ_i are listed in Table 1. The fundamental solutions U_{ij}^m and T_{ij}^m for the relaxation function given by Eq. (13) are obtained numerically by using elastic-viscoelas-

Table 1 The constants of Eq. (13)

λ_i(min)	E_i(MPa)
0.5×10^{14}	0.10817 $E+03$
0.5×10^{13}	0.12935 $E+03$
0.5×10^{12}	0.18168 $E+03$
0.5×10^{11}	0.23739 $E+03$
0.5×10^{10}	0.28994 $E+03$
0.5×10^{9}	0.32514 $E+03$
0.5×10^{8}	0.33116 $E+03$
0.5×10^{7}	0.30568 $E+03$
0.5×10^{6}	0.25760 $E+03$
0.5×10^{5}	0.20145 $E+03$
0.5×10^{4}	0.14720 $E+03$
0.5×10^{3}	0.10934 $E+03$
0.5×10^{2}	0.48615 $E+02$
0.5×10	0.15854 $E+03$
–	E_0=0.16876 $E+03$

tic correspondence principle. The detailed calculation procedure is provided in Lee (1995). The resulting expression for U_{ij}^m and T_{ij}^m is presented as follows:

$$\begin{aligned} U_{ij}^m(\boldsymbol{y},\ \boldsymbol{x};\ \xi) &= \frac{1}{16\pi R}[A_1(\xi)\,\delta_{ij}+A_2(\xi)\,R_{,i}R_{,j}]\,H(\xi) \\ T_{ij}^m(\boldsymbol{y},\ \boldsymbol{x};\ \xi) &= -\frac{A_3(\xi)}{8\pi R^2}[R_{,k}n_k(\boldsymbol{x})\,\delta_{ij}+n_i(\boldsymbol{x})\boldsymbol{R}_{,j}-n_j(\boldsymbol{x})\boldsymbol{R}_{,i}]\,H(\xi) \\ &\quad -\frac{A_4(\xi)}{8\pi R^2}3R_{,k}n_k(\boldsymbol{x})\,R_{,i}R_{,j}H(\xi) \end{aligned} \tag{14}$$

where $H(\xi)$ is the Heaviside unit step function, and

$$\begin{aligned} R_{,i} &= \frac{R_i}{R} \\ R_i &= x_i - y_i \\ R^2 &= R_iR_i \end{aligned} \tag{15}$$

y_i; coordinate of field point
x_i; coordinate of integration point

The coefficients $A_i(\xi)$ are obtained as follows:

$$A_1(\xi)=a_1^0+\sum_{i=1}^{28}a_1^i\exp(-c_1^i\xi)$$

$$A_2(\xi)=a_2^0+\sum_{i=1}^{28}a_2^i\exp(-c_2^i\xi)$$

$$A_3(\xi)=a_3^0+\sum_{i=1}^{14}a_3^i\exp(-c_3^i\xi)$$

$$A_4(\xi)=a_4^0+\sum_{i=1}^{14} a_4^i \exp(-c_4^i \xi) \quad (16)$$

The values of a_j^i and c_j^i are listed in Tables 2 and 3.

4. Numerical results

A suitable mesh density was determined for the analysis based upon the results of a convergence study for mesh refinement. The refined mesh was used near the interface corner. The boundary element discretization consisting of 60 line elements was employed. In this study, quadratic shape functions were used to describe both the geometric and functional variations.

Viscoelastic stress profiles are plotted along interface to investigate the nature of stresses. Fig. 2 shows the distribution of normal interface stress σ_{yy} on the interface. Except near the interface corner, this stress is approximately zero. A large gradient in σ_{yy} is observed in the vicinity of the free surface. Fig. 3 is a plot of shear stress τ_{xy} vs. x/L. This profile shows a stress singularity

Table 2 Numerical values of constants in $A_1(\xi)$ and $A_2(\xi)$ of Eq. (16)

a_1^i(MPa^{-1})	a_2^i(MPa^{-1})	c_1^i, c_2^i(min^{-1})
−0.10409 E-03	−0.10409 E-03	0.18946 E-00
−0.34529 E-04	−0.34529 E-04	0.19657 E-01
−0.81264 E-04	−0.81264 E-04	0.19221 E-02
−0.12016 E-03	−0.12016 E-03	0.18909 E-03
−0.18802 E-03	−0.18802 E-03	0.18423 E-04
−0.29187 E-03	−0.29187 E-03	0.17814 E-05
−0.45356 E-03	−0.45356 E-03	0.17088 E-06
−0.70416 E-03	−0.70416 E-03	0.16303 E-07
−0.10921 E-02	−0.10921 E-02	0.15534 E-08
−0.16925 E-02	−0.16925 E-02	0.14850 E-09
−0.26246 E-02	−0.26246 E-02	0.14292 E-10
−0.39079 E-02	−0.39079 E-02	0.14030 E-11
−0.60269 E-02	−0.60239 E-02	0.13663 E-12
−0.13776 E-01	−0.13773 E-01	0.11913 E-13
−0.71150 E-05	0.71150 E-05	0.19756 E+00
−0.22207 E-05	0.22207 E-05	0.19924 E-01
−0.50442 E-05	0.50442 E-05	0.19829 E-02
−0.69285 E-05	0.69285 E-05	0.19768 E-03
−0.97456 E-05	0.97456 E-05	0.19679 E-04
−0.12936 E-04	0.12936 E-04	0.19583 E-05
−0.16092 E-04	0.16092 E-04	0.19494 E-06
−0.18423 E-04	0.18423 E-04	0.19438 E-07
−0.19183 E-04	0.19183 E-04	0.19431 E-08
−0.18102 E-04	0.18102 E-04	0.19478 E-09
−0.15578 E-04	0.15580 E-04	0.19561 E-10
−0.12769 E-04	0.12630 E-04	0.19660 E-11
−0.89298 E-05	0.89281 E-05	0.19751 E-12
−0.77076 E-05	0.77061 E-05	0.19789 E-13
a_1^0=0.33335 E-01	a_2^0=0.32241 E-01	—

Table 3 Numerical values of constants in $A_3(\xi)$ and $A_4(\xi)$ of Eq. (16)

a_3^i	a_4^i	c_3^i, c_4^i ($\min^{-1}$)
0.18973 E-01	−0.18973 E-01	0.19756 E+00
0.59219 E-02	−0.59219 E-02	0.19924 E-01
0.13451 E-01	−0.13451 E-01	0.19829 E-02
0.18476 E-01	−0.18476 E-01	0.19768 E-03
0.25988 E-01	−0.25988 E-01	0.19679 E-04
0.34495 E-01	−0.34495 E-01	0.19583 E-05
0.42912 E-01	−0.42912 E-01	0.19494 E-06
0.49128 E-01	−0.49128 E-01	0.19438 E-07
0.51153 E-01	−0.51153 E-01	0.19431 E-08
0.48267 E-01	−0.48267 E-01	0.19478 E-09
0.41517 E-01	−0.41521 E-01	0.19561 E-10
0.33074 E-01	−0.32691 E-01	0.19660 E-11
0.24233 E-01	−0.24234 E-01	0.19751 E-12
0.20764 E-01	−0.20764 E-01	0.19789 E-13
a_3^0=0.33185 E-01	a_4^0=0.19664 E+01	—

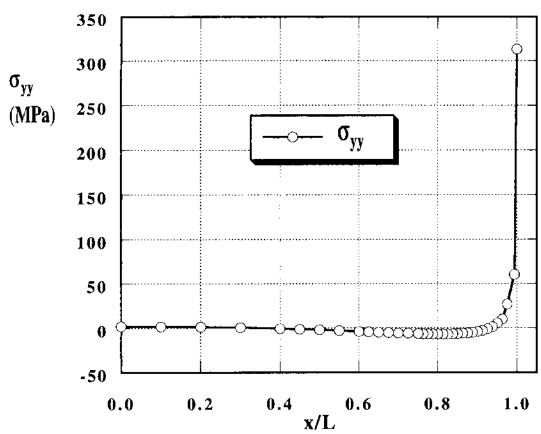

Fig. 2 Distribution of normal stress σ_{yy} on the interface at room temperature.

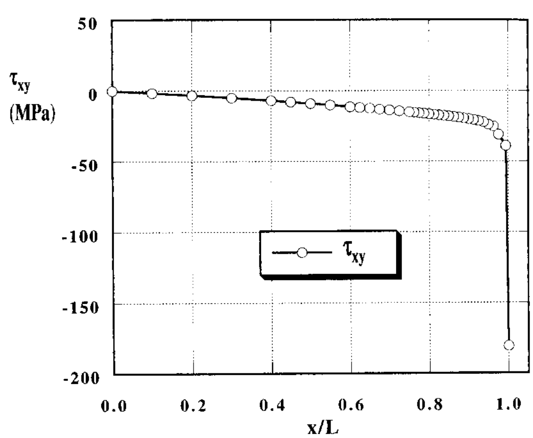

Fig. 3 Distribution of shear stress τ_{xy} on the interface at room temperature.

at interface corner. Figs. 2 and 3 suggest that the thermal stress singularity on the interface dominates a very small region relative to layer thickness for the case examined. It is not known, however, if the size of this region is large compared to that of intrinsic flaws.

5. Conclusions

The time-domain boundary element method was used to investigate the singular thermal stresses at the interface corner between the elastic fiber and the viscoelastic matrix of a unidirectional laminate due to cooling from cure temperature down to room temperature. Numerical results show that very large stress gradients are present at the interface corner and this stress singularity dominates a very small region relative to layer thickness. Since the exceedingly large stresses at the interface corner can not be borne by matrix materials, local yielding or fiber-matrix debonding may occur in the vicinity of free surface.

References

Griffin, Jr., O.H. (1983), "Three-dimensional curing stresses in symmetric cross-ply laminates with temperature-dependent properties," *J. of Composite Materials*, **17**, 449-463.

Hahn, H.T. (1976), "Residual stresses in polymer matrix composite laminates", *J. Composite Materials*, **10**, 266-277.

Hahn, H.T. and Pagano, N.J. (1975), "Curing stresses in composite laminates", *J. Composite Materials*, **9**, 91-106.

Kim, R.Y. and Hahn, H.T. (1979), "Effect of curing stresses on the first ply-failure in composite laminates", *J. Composite Materials*, **13**, 2-14.

Lee, S.S. (1995), "Time-domain boundary element analysis of viscoelastic solids using realistic relaxation functions," *Computers & Structures*, **55**, 1027-1036.

Lee, S.S. and Sohn, Y.S. (1994), "Viscoelastic analysis of residual stresses in a unidirectional laminate," *Structural Engineering and Mechanics*, **2**, 383-393.

Lee, S.S. and Westmann, R.A. (1995), "Application of high-order quadrature rules to time-domain boundary element analysis of viscoelasticity," *Int. J. Numerical Methods in Engineering*, **38**, 607-629.

Roy, A. and Murthy, P.N. (1976), "Viscoelastic analysis of the residual stress in glass fiber reinforced plastics," *Fiber Science and Technology*, **9**, 81-101.

Weitsman, Y. (1979), "Residual thermal stresses due to cool-down of epoxy-resin composite", *J. Appl. Mech.*, **46**, 563-567.

Weitsman, Y. and Harper, B.D. (1982), "Optimal cooling of cross-ply composite laminates and adhesive joints," *J. Applied Mechanics*, **49**, 735-739.